Neuron
Article

# Extracellular Calcium Controls Background Current and Neuronal Excitability via an UNC79-UNC80-NALCN Cation Channel Complex

Boxun Lu,[1] Qi Zhang,[1] Haikun Wang,[1] Yan Wang,[1] Manabu Nakayama,[2] and Dejian Ren[1,*]
[1]Department of Biology, University of Pennsylvania, Philadelphia, PA 19104, USA
[2]Department of Human Genome Research, Kazusa DNA Research Institute, Kisarazu, Chiba 292-0818, Japan
*Correspondence: dren@sas.upenn.edu
DOI 10.1016/j.neuron.2010.09.014

## SUMMARY

**In contrast to its extensively studied intracellular roles, the molecular mechanisms by which extracellular $Ca^{2+}$ regulates the basal excitability of neurons are unclear. One mechanism is believed to be through $Ca^{2+}$'s interaction with the negative charges on the cell membrane (the charge screening effect). Here we show that, in cultured hippocampal neurons, lowering $[Ca^{2+}]_e$ activates a NALCN channel-dependent $Na^+$-leak current ($I_{L\text{-}Na}$). The coupling between $[Ca^{2+}]_e$ and NALCN requires a $Ca^{2+}$-sensing G protein-coupled receptor, an activation of G-proteins, an UNC80 protein that bridges NALCN to a large novel protein UNC79 in the same complex, and the last amino acid of NALCN's intracellular tail. In neurons from *nalcn* and *unc79* knockout mice, $I_{L\text{-}Na}$ is insensitive to changes in $[Ca^{2+}]_e$, and reducing $[Ca^{2+}]_e$ fails to elicit the excitatory effects seen in the wild-type. Therefore, extracellular $Ca^{2+}$ influences neuronal excitability through the UNC79-UNC80-NALCN complex in a G protein-dependent fashion.**

## INTRODUCTION

$Na^+$, $K^+$, and $Ca^{2+}$ each regulate the excitability of neurons. The effect of extracellular $Na^+$ and $K^+$ can largely be explained by the permeability of the cell to these ions ($P_{Na}$ and $P_K$). $P_{Na}$ is normally a fraction of $P_K$ at rest, at ~4% in the squid giant axon (Hodgkin and Katz, 1949), which results in a resting membrane potential closer to that of the equilibrium (Nernst) potential of $K^+$ ($E_K$) than to $E_{Na}$. Many $K^+$ channels, such as the two-pore $K_{2P}$ leak channels, contribute to the resting $P_K$ (Goldstein et al., 2005). At rest, $Na^+$ is believed to leak into neurons through voltage-gated $Na^+$ channels via the window conductance, hyperpolarization-activated channels (HCNs), $Na^+$-coupled transporters, and the recently characterized $Na^+$-leak channel NALCN (Lu et al., 2007; Nicholls et al., 2001). However, the way in which extracellular $Ca^{2+}$ influences the resting excitability is poorly understood at the molecular level. This lies in sharp contrast to the extensively studied roles of intracellular $Ca^{2+}$ in physiological functions including muscle contraction, hormone secretion, synaptic transmission, and gene expression (Clapham, 2007).

Under both physiological and pathological conditions, $[Ca^{2+}]_e$ can drop significantly in brain regions such as the hippocampus, neocortex, and cerebellum. For example, repetitive electrical or chemical stimulation in areas where extracellular space is limited can cause $[Ca^{2+}]_e$ to decrease from ~1.3 to 0.1 mM, presumably as a result of the movement of extracellular $Ca^{2+}$ into cells (Benninger et al., 1980; Heinemann and Pumain, 1980; Krnjevic et al., 1982; Nicholson et al., 1977; Pumain et al., 1985). Single stimuli are also believed to lead to $Ca^{2+}$ depletion in microdomains such as the synaptic cleft (Borst and Sakmann, 1999; Rusakov and Fine, 2003; Stanley, 2000). In the cerebral cortex of the cat during slow wave sleep, $[Ca^{2+}]_e$ levels have been reported to oscillate between 1.18 and 0.85 mM, in phase with membrane potential oscillation in this region, and $[Ca^{2+}]_e$ can drop further, below 0.5 mM, if such cortical oscillation evolves into a spike-wave seizure (Amzica et al., 2002). Large drops in $[Ca^{2+}]_e$ are also observed in a variety of other models of seizure, hypoxia, ischemia, and trauma (Heinemann et al., 1986; Morris and Trippenbach, 1993; Nilsson et al., 1993; Silver and Erecinska, 1990).

Unlike $Na^+$ and $K^+$, extracellular $Ca^{2+}$ negatively influences neuronal excitability: a decrease in $[Na^+]_e$ or $[K^+]_e$ normally suppresses neuronal excitability, whereas a decrease in $[Ca^{2+}]_e$ usually excites neurons (Hille, 2001; Nicholls et al., 2001). Several mechanisms have been proposed to explain this negative regulation. First, $Ca^{2+}$ neutralizes negative charges on the cell membrane. Reduction in such charge-screening effects can shift the voltage dependences of biophysical properties (activation and inactivation, for example) of many ion channels such as $Na_V$s and $K_V$s toward hyperpolarization (Frankenhaeuser and Hodgkin, 1957; Hille, 2001). In addition, $Ca^{2+}$ can directly interact with channel gating machinery (Armstrong and Cota, 1991). A reduction in $[Ca^{2+}]_e$ also activates depolarizing, nonselective cation currents in cell bodies and nerve terminals (Formenti et al., 2001; Hablitz et al., 1986; Smith et al., 2004; Xiong et al., 1997). The molecular identities of the channels responsible for the currents, the mechanisms by which $[Ca^{2+}]_e$ change is coupled to channel opening, and the role of these channels in the regulation of neuronal excitability by $[Ca^{2+}]_e$ remain largely unknown.

NALCN ($Na^+$-leak channel, nonselective; [Lu et al., 2007]) is a member of the 24-transmembrane-spanning (24 TM) ion

channel family, which also includes 10 voltage-gated $Ca^{2+}$ channels ($Ca_V$s) and 10 $Na^+$-selective channels ($Na_V1.1$–$1.9$ and $Na_X$) (Snutch and Monteil, 2007; Yu et al., 2005). The protein is unique in that its S4 transmembrane segments lack some of the charged residues (K and R) found at every third position in the S4s of the $Na_V$, $Ca_V$, and $K_V$ channels. In addition, its pore filter regions have an EEKE motif, a mixture between the EEEE found in the $Ca_V$s and the DEKA of $Na_V$s (Lee et al., 1999). Consistent with these unique structural features, NALCN is the only nonselective, noninactivating, voltage-independent channel among the family's 21 members (Lu et al., 2007). Unlike some of the $Ca_V$s and $Na_V$s, the subunit composition of NALCN has not been determined. NALCN is widely expressed in the nervous system. In cultured hippocampal neurons, it contributes the major TTX- and Cs-resistant $Na^+$ leak at voltages close to the resting membrane potential. Mice with a targeted disruption in *nalcn* have severely disrupted respiratory rhythms and die within 24 hr of birth (Lu et al., 2007). Mutations in the NALCN homolog genes in *Drosophila melanogaster* (*Na*) and *Caenorhabditis elegans* (*Nca*) lead to defects in locomotion, anesthetic sensitivity, rhythmic behaviors, and synaptic function (Humphrey et al., 2007; Jospin et al., 2007; Pierce-Shimomura et al., 2008; Yeh et al., 2008). In addition, mutant screening suggests that *nalcn* genetically interacts with other genes such as *unc-79* and *unc-80*, whose mammalian counterparts are *unc79* and *unc80*, respectively (Humphrey et al., 2007; Jospin et al., 2007; Yeh et al., 2008). It is not known by what means NALCN, UNC79, and UNC80 might functionally interact in the brain.

In this study, we found that, in hippocampal neurons, extracellular $Ca^{2+}$ regulates neuronal excitability by controlling the sizes of the NALCN-dependent $Na^+$-leak current. We identify NALCN as the cation channel that is activated by a reduction in $[Ca^{2+}]_e$. Its activation in neurons requires UNC79 and UNC80, where UNC79 indirectly associates with NALCN through its interaction with UNC80. The coupling between $[Ca^{2+}]_e$ and the channel occurs via a $[Ca^{2+}]_e$-sensing G protein-coupled receptor (GPCR) and requires the intracellular carboxy terminus of the channel.

## RESULTS

### NALCN Is Required for the Excitatory Effects of a Reduction in $[Ca^{2+}]_e$

In many types of neurons, a decrease of $[Ca^{2+}]_e$ excites neurons via mechanisms that are poorly understood (Burgo et al., 2003; Chinopoulos et al., 2007; Formenti et al., 2001; Xiong et al., 1997). To determine whether NALCN protein might be involved in the low $[Ca^{2+}]_e$-induced excitation, we compared hippocampal neurons cultured from wild-type with those from mice deficient in NALCN ($nalcn^{-/-}$) using current clamp. In the wild-type neurons, lowering $[Ca^{2+}]_e$ from 1.2 mM to 0.5 mM increased the frequencies of firing elicited by depolarizing current injection, and sometimes converted a nonfiring neuron to a firing one (Figures 1A and 1C; see Figure S1 available online). Surprisingly, this low $[Ca^{2+}]_e$ response is largely missing in the $nalcn^{-/-}$ neurons (Figures 1B and 1C; Figure S1). The $[Ca^{2+}]_e$ response could be partially restored by transfecting NALCN cDNA back to the $nalcn^{-/-}$ mutant neurons (Figure S1).

### Extracellular $Ca^{2+}$ Controls the Sizes of the NALCN-dependent $Na^+$-leak Current

A major mechanism by which $[Ca^{2+}]_e$ regulates the basal excitability of neurons has been thought to be through the ion's charge screening effect on the membrane surface (Frankenhaeuser and Hodgkin, 1957; Hille, 2001). Our finding that the low $[Ca^{2+}]_e$-induced excitation requires NALCN was thus unexpected because the protein forms a nonselective ion channel responsible for the $Cs^+$- and TTX-insensitive background $Na^+$ leak current ($I_{L\text{-}Na}$) at resting (Lu et al., 2007). To test whether extracellular $Ca^{2+}$ instead influences neuronal excitability by controlling $I_{L\text{-}Na}$, we measured the current in the presence of TTX and $Cs^+$, which we used to block the contribution from $Na_V$s and HCNs, respectively. We further isolated the small $Na^+$ leak current by measuring the difference ($\Delta I_{L\text{-}Na}$) between holding currents obtained in baths containing 140 mM and 14 mM $Na^+$ (Lu et al., 2007). When $[Ca^{2+}]_e$ was lowered from 2 mM to 0.1 mM, a large increase (6.5 ± 0.7-fold, n = 5) of $\Delta I_{L\text{-}Na}$ was observed (Figures 2A and 2B). A further decrease of $[Ca^{2+}]_e$ to 0.01 mM led to a 10.7 ± 0.7-fold (n = 6) increase. Thus, the $Na^+$ leak current faithfully reflected $[Ca^{2+}]_e$ changes in a wide range between 0.01 and 2 mM (Figure 2B); lowering $[Ca^{2+}]_e$ increases the $Na^+$ leak and leads to an inward current ($I_{LCA}$). Similar to currents generated by NALCN ($I_{NALCN}$) (Lu et al., 2007), the low $[Ca^{2+}]_e$-activated current $I_{LCA}$ was blocked by 10 μM $Gd^{3+}$ and 1 mM verapamil (not shown).

In contrast to wild-type cells, $nalcn^{-/-}$ hippocampal neurons lacked an $I_{LCA}$ when $[Ca^{2+}]_e$ was lowered to 0.1 mM (Figures 2C and 2D). Transfection of NALCN cDNA, but not empty vector, into the $nalcn^{-/-}$ neurons restored the current (Figures 2E and 2F). These data suggest that $I_{LCA}$ is dependent on NALCN.

Like in the $nalcn^{-/-}$ neurons, transfection of NALCN cDNA into SH-SY5Y, a neuroblastoma cell line that lacks endogenous $I_{LCA}$, also reconstituted an $I_{LCA}$ (Figure S2A). The I-V relationship (Figure S2D) of the current was similar to that of the native $I_{LCA}$ currents that have been recorded in neurons (Xiong et al., 1997).

Currents similar to the NALCN-generated $I_{LCA}$ we recorded have also been postulated to arise via TRPM7 (MacDonald et al., 2006; Wei et al., 2007), a ubiquitously expressed TRP channel that opens when the intracellular $[Mg^{2+}]$ is artificially low (Kozak and Cahalan, 2003; Nadler et al., 2001). Under our $I_{LCA}$ recording conditions, with 2 mM free $Mg^{2+}$ inside and 1 mM free $Mg^{2+}$ outside the cells, TRPM7 transfected into SH-SY5Y generated essentially no $I_{LCA}$ (0.8 ± 1.7 pA, n = 6; at −80 mV; compared to −235.6 ± 39.6 pA in the NALCN-transfected cells, n = 13). When no $Mg^{2+}$ was included in the pipette solution, TRPM7 generated a current with an outwardly rectifying I-V relationship similar to that of the TRPM7 currents that have been recorded in many other cells (Kozak and Cahalan, 2003; Monteilh-Zoller et al., 2003; Nadler et al., 2001; Runnels et al., 2001), but distinct from those of the NALCN currents (Lu et al., 2007; Lu et al., 2009) and $I_{LCA}$ currents (Xiong et al., 1997), both of which have a linear I-V relationship and are blocked by 10 μM $Gd^{3+}$. The TRPM7 current was essentially insensitive to a drop in $[Ca^{2+}]_e$ from 2.0 mM to 0.1 mM (−4.5 ± 3.6 pA, n = 5), unless $[Ca^{2+}]_e$ was further dropped to 0.01 mM (−11.9 ± 10.1 pA, n = 4). These data suggest that, although TRPM7 may

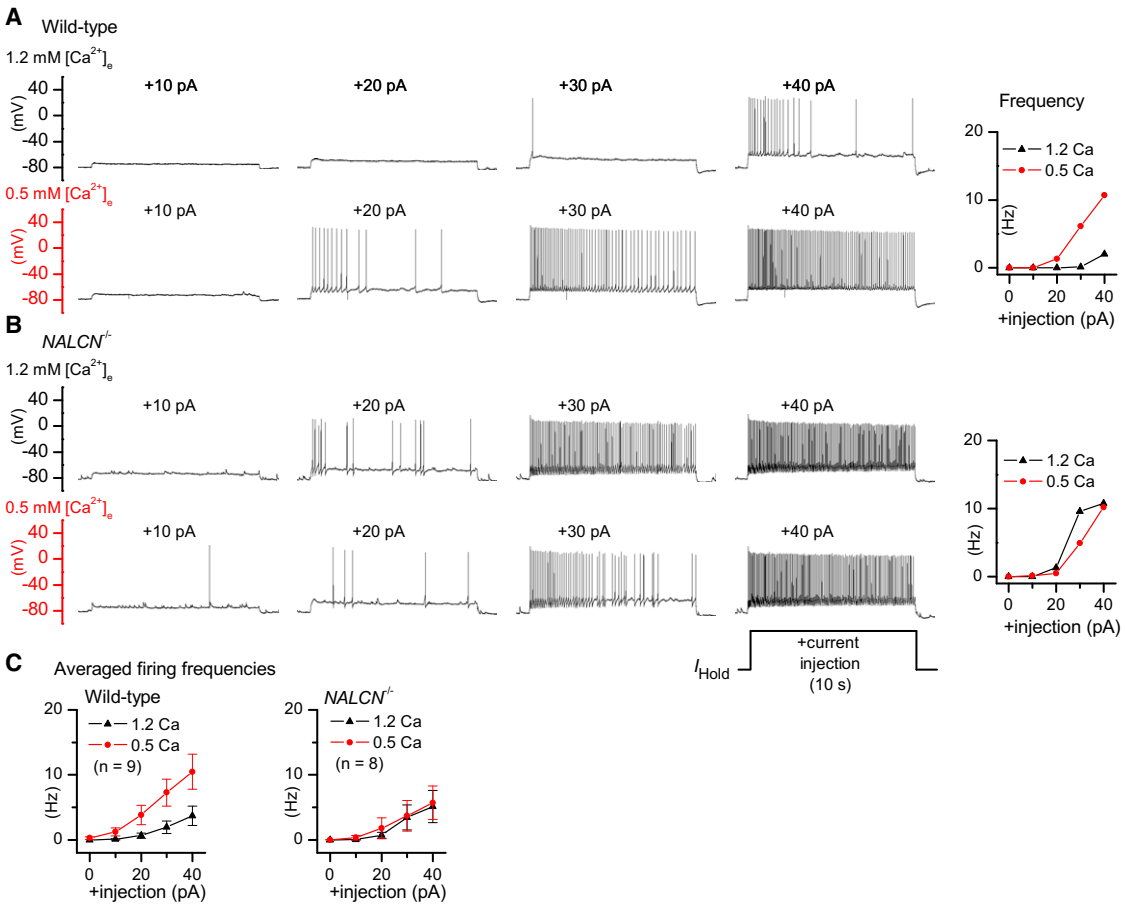


**Figure 1. Dependence of the Excitatory Action of Low $[Ca^{2+}]_e$ on NALCN**

A hyperpolarizing holding current ($I_{Hold}$, −45 pA in the neuron in (A); −30 pA in (B); and −33.7 ± 11.0 pA (wild-type) and −14.8 ± 5.0 pA (*NALCN*$^{-/-}$) in (C) was injected to bring each neuron's steady membrane potential to −80 mV in 1.2 mM $Ca^{2+}$-containing bath. Pulses (10 s, as illustrated in lower right in B) of additional depolarizing currents with increasing amplitudes (+10 to +40 pA; "+injection" in the x axes) superimposed on the holding currents ($I_{Hold}$) were injected every 50 s. (A and B) Examples of current-clamp recordings from a wild-type (A) and a *nalcn* mutant neuron (B) in baths containing 1.2 mM (upper traces) or 0.5 mM (lower traces) $Ca^{2+}$. Firing frequencies of the neurons during the 10 s depolarizing pulses are plotted in the right panels. (C) Statistics of firing frequencies from wild-type (*left*) and *nalcn*$^{-/-}$ neurons (*right*). Error bars represent mean and standard error of the mean (SEM). See also Figure S1.

account for a small portion under artificially low $[Mg^{2+}]_i$, $[Mg^{2+}]_e$, and $[Ca^{2+}]_e$, $I_{LCA}$ occurs largely through NALCN.

## The Sensitivity of the NALCN Current to $[Ca^{2+}]_e$ Is Dependent on the Carboxy-Terminal Tail of NALCN Protein

To determine the structural requirements of NALCN protein for the channel current's ($I_{NALCN}$) sensitivity to $[Ca^{2+}]_e$, we deleted residues in the NALCN carboxy terminus, one of the two large, presumably intracellular domains (the other one being the loop connecting repeats II and III, each of which contains ~280 amino acids [aa]). The carboxy terminus consists of two fragments highly conserved among vertebrates, separated by another that is less conserved (Figure 3A). A form of NALCN in which the last 202 aa were deleted was nonfunctional and failed to generate a basal $Na^+$ leak current (not shown). A mutant with a shorter deletion (101 aa, Δ1638–1738) generated a basal $Na^+$ leak current ($\Delta I_{L\text{-}Na}$) when transfected into SH-SY5Y cells or *nalcn*$^{-/-}$ hippocampal neurons, but the current was not sensitive to $[Ca^{2+}]_e$ changes between 2 mM and 0.1 mM (Figure 3C; Figure S3), suggesting that the last 101 amino acids are required for the sensitivity of $I_{NALCN}$ to $[Ca^{2+}]_e$. Results from additional deletions (Δ1657–1699 and Δ1623–1699) suggest that the non-conserved fragment is less important for the $[Ca^{2+}]_e$ sensitivity (Figures 3B and 3C). In contrast, the second highly conserved fragment is strictly required (see Δ1733–1738 and Δ1724–1732) (Figures 3B and 3C). In addition, deleting the last amino acid (I1738; Δ1738) rendered the channel largely insensitive to changes in $[Ca^{2+}]_e$ (Figures 3B and 3C).

## Synergism between Low $[Ca^{2+}]_e$ and the Neuropeptide Substance P in NALCN Activation

NALCN is also activated by substance P (SP) in ~50% of the cultured hippocampal neurons (Lu et al., 2009). If lowered $[Ca^{2+}]_e$ and SP acted independently on the same target, the two would be expected to exert a synergistic effect. Consistent

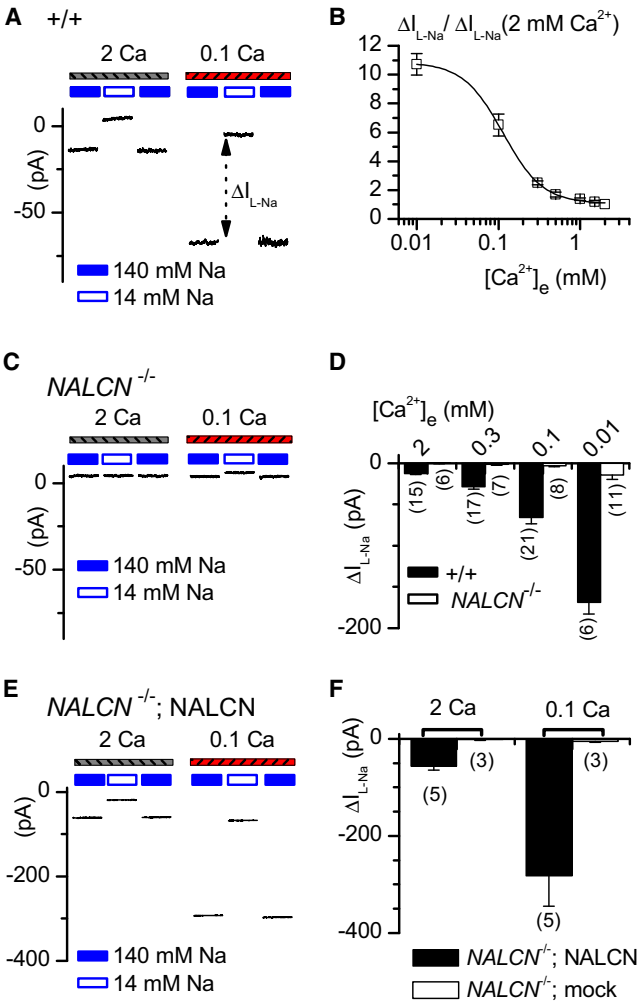


**Figure 2. Control of Resting $Na^+$ Leak Current by Extracellular $Ca^{2+}$ in Cultured Hippocampal Neurons**

(A) Representative holding currents at –68 mV in a wild-type (+/+) neuron. $Na^+$-leak current is presented as $\Delta I_{L\text{-}Na}$ (indicated by the double arrow), defined as the difference between holding currents in 140 mM (solid bar) and 14 mM (open bar) $Na^+$-containing baths. A 0.25 s recording is shown for each condition. $\Delta I_{L\text{-}Na}$ increased when $[Ca^{2+}]_e$ was switched from 2 mM (indicated by the hatched bar labeled 2 Ca) to 0.1 mM (0.1 Ca).

(B) $\Delta I_{L\text{-}Na}$ in wild-type neurons measured at various $[Ca^{2+}]_e$ normalized to that measured with 2 mM $[Ca^{2+}]_e$ ($n \geq 5$).

(C) Similar to (A), but from a *nalcn*$^{-/-}$ neuron.

(D) Comparison of $\Delta I_{L\text{-}Na}$ between wild-type (+/+) and *nalcn*$^{-/-}$ neurons at a range of $[Ca^{2+}]_e$, as indicated. The number of cells for each condition is indicated in parentheses.

(E) Representative $\Delta I_{L\text{-}Na}$ restored by NALCN cDNA transfection into the *nalcn*$^{-/-}$ neurons.

(F) Summary of $\Delta I_{L\text{-}Na}$ generated by NALCN or mock (empty vector) transfection in 2 mM and 0.1 mM $[Ca^{2+}]_e$ (mean ± SEM). See also Figure S2.

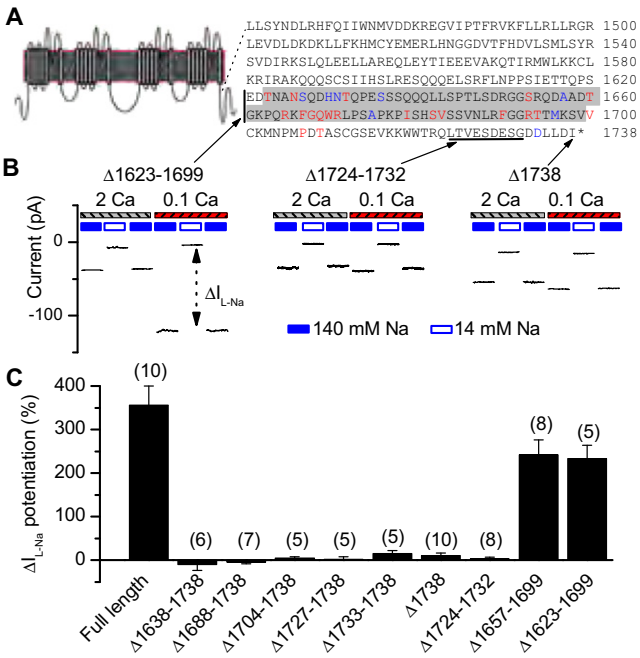


**Figure 3. Dependence of Low $[Ca^{2+}]_e$-activated Current ($I_{LCA}$) on the Carboxy-Terminal Residues of NALCN**

(A) Schematic illustration of the location of the NALCN C-terminal mutants. The C-terminal sequences (from the rat isoform, accession number NP_705894) are shown (right). Nonconserved (red) and conserved (blue) amino acid substitutions in the chicken isoform (accession number XP_416967) are highlighted. Shadowed sequences indicate sequence nonessential to $I_{LCA}$ (deleted in Δ1623–1699).

(B) Representative $\Delta I_{L\text{-}Na}$ recordings from SH-SY5Y cells transfected with NALCN deletion mutants Δ1623–1699 (with amino acids 1623–1699 deleted), Δ1724–1732 and Δ1738.

(C) Summary of potentiation of $\Delta I_{L\text{-}Na}$ by lowering $[Ca^{2+}]_e$ from 2 mM to 0.1 mM, defined as percentage of increase ([$\Delta I_{L\text{-}Na}$ in 0.1 mM $Ca^{2+}$ – $\Delta I_{L\text{-}Na}$ in 2 mM $Ca^{2+}$]/$\Delta I_{L\text{-}Na}$ in 2 mM $Ca^{2+}$). Data from transfected *nalcn*$^{-/-}$ and SH-SY5Y cells were pooled. Measurements from the five full-length NALCN-transfected neurons used in Figure 2F were also included for comparison. See Figure S3 for the averaged sizes of $\Delta I_{L\text{-}Na}$ in 2 mM and 0.1 mM $Ca^{2+}$-containing baths. Error bars represent mean and SEM.

with this prediction, in wild-type neurons that had SP-activated current $I_{SP}$, $I_{LCA}$ was strongly potentiated by the SP application (7.6 ± 1.5 fold, n = 19; Figure 4). In *nalcn*$^{-/-}$ neurons, applying both stimuli simultaneously failed to activate significant current. Transfection of NALCN cDNA into the *nalcn*$^{-/-}$ neurons restored the synergistic effect. A truncated NALCN that lacked the carboxy terminus (Δ1638–1738) restored the SP-activated current (−172 ± 89 pA, n = 12), but the current was largely insensitive to the $[Ca^{2+}]_e$ change (Figure 4B). The synergism between lowering $[Ca^{2+}]_e$ and SP application further supports the hypothesis that $I_{LCA}$ is derived from NALCN.

## NALCN Associates with UNC79 via UNC80 in the Brain, and UNC79 Influences UNC80 Protein Levels

Our finding that the sensitivity of $I_{NALCN}$ to $[Ca^{2+}]_e$ requires the last amino acids in the intracellular tail of the NALCN protein suggests that the coupling between $[Ca^{2+}]_e$ changes and NALCN involves an intracellular mechanism. In addition, unlike in neurons and SH-SY5Y neuroblastoma cells, overexpression of NALCN alone in HEK293T fibroblasts generates a current that is insensitive to $[Ca^{2+}]_e$ changes (data not shown), suggesting that the sensitivity to $[Ca^{2+}]_e$ of NALCN in neurons may require

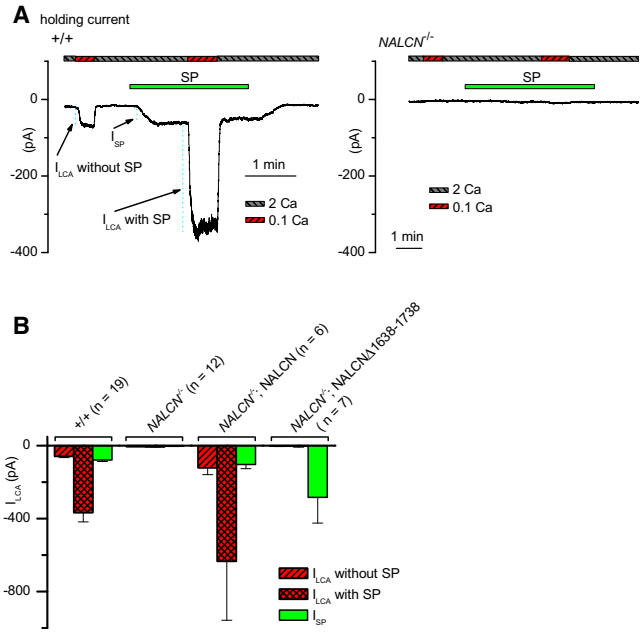


**Figure 4. Synergism between Low $[Ca^{2+}]_e$ and Substance P**

(A) Representative recordings of $I_{LCA}$ in the presence and absence of substance P (1 μM), from a wild-type neuron cultured on pre-plated glial cells (left), or a *nalcn*$^{-/-}$ neuron cultured under the same conditions (right).

(B) Average $I_{LCA}$ of wild-type (+/+), *NALCN*$^{-/-}$, and full-length (*NALCN*$^{-/-}$; NALCN) or carboxy-terminal truncated (Δ1638–1738) NALCN cDNA-transfected *nalcn*$^{-/-}$ neurons in the presence or absence of SP. For the wild-type or transfected neurons, only cells with >20 pA SP-activated current ($I_{SP}$, measured under 2 mM $[Ca^{2+}]_e$ as illustrated by an arrow in (A) were selected for analysis. *nalcn*$^{-/-}$ neurons had no detectable $I_{SP}$. Error bars represent mean and SEM.

interaction with other intracellular proteins. Recent genetic studies in the fruit fly *Drosophila melanogaster* and the nematode *Caenorhabditis elegans* suggest that the *nalcn* gene interacts with other genes, including *unc79* and *unc80*, which encode two proteins that appear to be intracellular (Humphrey et al., 2007; Jospin et al., 2007; Pierce-Shimomura et al., 2008; Yeh et al., 2008). In the mouse brain, UNC80 associates with NALCN (Lu et al., 2009). To test whether UNC79 is also a part of the NALCN protein complex, we cloned mammalian UNC79 homologs from human and mouse brains, and developed a polyclonal antibody against them. The predicted mouse and human UNC79 proteins are 94% identical. They have 30%–50% identity with their homologs from invertebrates such as fruit flies, soil worms, and sea urchins. Despite its large size (mouse, 2657 aa; human, 2654 aa), UNC79 has no similarity to domains with known function. Immunoprecipitating UNC79 from mouse brain also precipitated NALCN (Figure 5A, lane 1) and UNC80 (Figure 5A, lane 4), suggesting that the three proteins are physically associated in the brain.

In HEK293T cells cotransfected with an HA-tagged UNC79 (HA-UNC79) and a GFP-tagged UNC80 (GFP-UNC80), immunoprecipitating GFP-UNC80 with an anti-GFP antibody also brought down HA-UNC79 (Figure 5B, lane 1), suggesting that the interaction between UNC79 and UNC80 does not require NALCN. Unlike UNC80 (Lu et al., 2009), UNC79 does not seem to interact with NALCN directly, as immunoprecipitating either of NALCN (Figure 5B, lane 3) or UNC79 (Figure 5B, lane 6) did not bring down the other when they were cotransfected in the absence of UNC80. When UNC80 was added to the transfection, however, immunoprecipitating NALCN also brought down UNC79 (Figure 5B, lane 4) and vice versa (Figure 5B, lane 7). These data suggest an UNC79-UNC80- NALCN complex model in which UNC79 interacts with UNC80, which in turn associates with the pore-forming subunit (NALCN) of the channel complex (see Figure S7).

Elimination of an ion channel subunit can lead to instability of another component in the same complex (e.g., (Liu et al., 2007; Wang et al., 2009)). We examined the protein levels of UNC80 and NALCN in *unc79* (previous name KIAA1409 [Nakayama et al., 2006]) knockout mice, which have phenotypes similar to those of the *nalcn* mutant (Lu et al., 2007). The anti-UNC79 antibody recognized a specific protein band from wild-type brain (Figure 5C, lane WT), with a molecular weight close to that of the recombinant protein expressed in HEK293T cells, but this band was not detected in brain tissue from *unc79* knockout mice (Figure 5C, lane KO). In the *unc79* knockout, UNC80 protein was also undetectable (Figure 5D), but NALCN was present (Figure 5E, input). Consistent with the absence of both UNC79 and UNC80 in the *unc79* mutant, antibodies against UNC79 or UNC80 did not immunoprecipitate NALCN from the *unc79* KO brains, whereas they did in the wild-type (Figure 5E).

## UNC80 Is Essential for the NALCN's $[Ca^{2+}]_e$ Sensitivity

In the presence of 2 mM $Ca^{2+}$ in the bath, there was no obvious difference between $\Delta I_{L\text{-}Na}$ amplitudes in wild-type and *unc79*$^{-/-}$ hippocampal neurons (Figures 6A and 6D). $\Delta I_{L\text{-}Na}$ was largely absent in the *nalcn* knockout (data not shown; see also Figure 2D and Lu et al. [2007]). Together, these data suggest that NALCN can form a basal $Na^+$-leak channel without an absolute requirement for UNC79, and perhaps also UNC80.

$I_{NALCN}$ in the absence of UNC79 and UNC80, as recorded from the *unc79*$^{-/-}$ hippocampal neurons, however, was largely insensitive to changes in $[Ca^{2+}]_e$ (Figures 6A and 6D). Transfection of UNC79 cDNA into the *unc79*$^{-/-}$ hippocampal neurons restored the sensitivity to $[Ca^{2+}]_e$ of $I_{NALCN}$ (Figures 6B and 6D). Furthermore, on the *unc79*$^{-/-}$ background, overexpression of UNC80 alone with a strong CMV promoter in cultured neurons could bypass the requirement for UNC79 and rescue the $[Ca^{2+}]_e$ sensitivity (Figures 6C and 6D). Thus, the $[Ca^{2+}]_e$ sensitivity of $I_{NALCN}$ is dependent on UNC80, whereas UNC79 contributes to the sensitivity, perhaps indirectly, by affecting the UNC80 protein level.

Similar to *nalcn*$^{-/-}$ neurons (Figure 1), *unc79*$^{-/-}$ neurons were not excited by a $[Ca^{2+}]_e$ drop to 0.5 mM (Figure S4). In wild-type neurons, further lowering $[Ca^{2+}]_e$ down to 0.1 mM also led to a large depolarization of the membrane potential (+15.3 ± 3.1 mV, n = 14), in addition to an increase of firing frequencies (Figures 7A and 7C). This much more drastic effect on the firing properties of lowering $[Ca^{2+}]_e$ to 0.1 mM (Figure 7) than that by lowering $[Ca^{2+}]_e$ to 0.5 mM (Figure 1) is consistent with the finding that $\Delta I_{L\text{-}Na}$ is less sensitive to fluctuations of $[Ca^{2+}]_e$ at 1.2 mM than at 0.1 mM (Figure 2). The depolarization observed

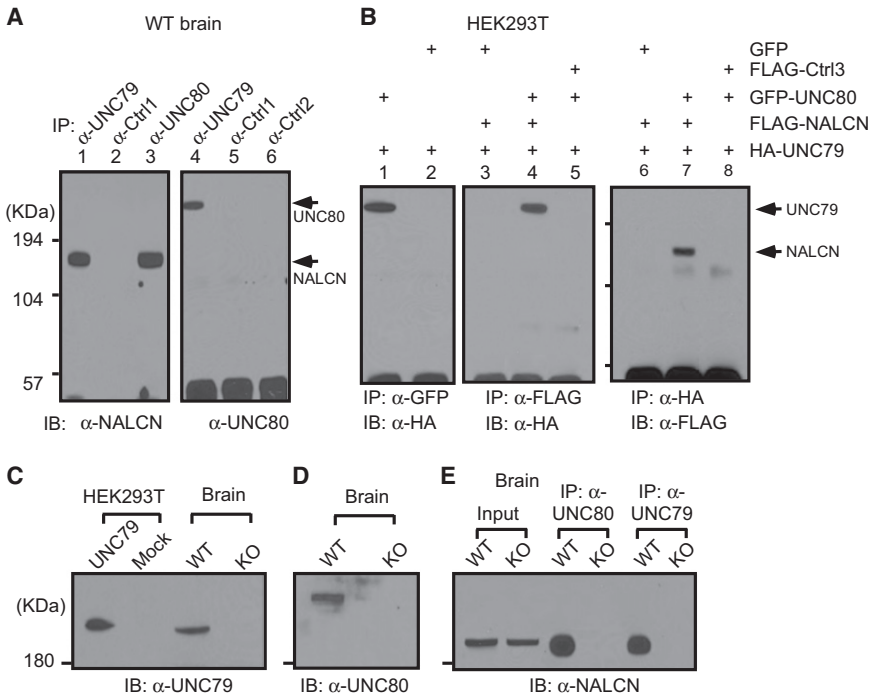


**Figure 5. UNC79 Forms a Complex with NALCN via Its Interaction with UNC80 in the Brain and Influences UNC80 Protein Level**

(A) Association of NALCN, UNC79, and UNC80 in the brain. Total mouse brain protein was immunoprecipitated (IP) with the indicated antibodies and blotted (IB) with anti-NALCN (left) or anti-UNC80 (right) antibodies. Anti-HA (α-Ctrl1) and anti-CATSPER1 (α-Ctrl2) were used as control antibodies for specificity.

(B) Association of UNC79 with the NALCN complex via its interaction with UNC80. Lysates from HEK293T cells transfected with the indicated combinations of plasmids were immunoprecipitated and blotted with indicated antibodies (lanes 1–2 and lanes 3–5 are from two separate gels). A FLAG-tagged transmembrane protein, CATSPERβ (FLAG-Ctrl3), was used as a control.

(C) Western blot using total brain protein from wild-type (WT) and *unc79* knockout (KO), showing the recognition of native UNC79 protein by the anti-UNC79 antibody. Cell lysates from HEK293T cells transfected with UNC79 cDNA or empty vector (mock) were loaded for molecular weight comparison and assessment of antibody specificity.

(D) Western blot showing absence of detectable UNC80 protein in the *unc79* knockout brain.

(E) Western blot with anti-NALCN showing NALCN protein in the *unc79* KO (left two lanes). Immunoprecipitating with anti-UNC79 or anti-UNC80 failed to precipitate NALCN in the KO because of the absence of UNC79 and UNC80 in the mutant. See also Figure S7 for a model of the interaction among NALCN, UNC79 and UNC80.

in the wild-type neurons by lowering $[Ca^{2+}]_e$ to 0.1 mM was largely absent in the *nalcn*$^{-/-}$ (+2.1 ± 0.6 mV, n = 12) or *unc79*$^{-/-}$ (+0.5 ± 1.0 mV, n = 15) mutant neurons (Figure 7).

## The Control of $I_{NALCN}$ by $[Ca^{2+}]_e$ Is through a G Protein-Dependent Signaling Pathway

How does a decrease in $[Ca^{2+}]_e$ "activate" NALCN channel and excite neurons? The monovalent currents through $Ca_V$ and several TRP channels are also $Ca^{2+}$-sensitive when $[Ca^{2+}]_e$ is artificially low, in the micromolar range (Almers and McCleskey, 1984; Hess et al., 1986; Owsianik et al., 2006). The major mechanism underlying this sensitivity is through a blockade of $Ca^{2+}$ in the channel pore from outside the cells; lowering $[Ca^{2+}]_e$ below 1 μM removes the blockade (Yang et al., 1993). However, it is unlikely that a similar pore-block mechanism accounts for the $[Ca^{2+}]_e$ sensitivity of NALCN at the more physiologically relevant, sub-mM $[Ca^{2+}]_e$ levels, since the channel expressed in HEK293T fibroblast cells is largely insensitive to $[Ca^{2+}]_e$ drops, as well as the fact that its $[Ca^{2+}]_e$ sensitivity requires NALCN's intracellular C-terminal tail and the presumably intracellular protein UNC80.

We tested whether G proteins could act as an intracellular transducer to couple the $[Ca^{2+}]_e$ signal to the NALCN-UNC80 complex. Upon cell dialysis with a pipette solution containing GTPγS, a nonhydrolyzable GTP analog that constitutively activates G proteins, lowering $[Ca^{2+}]_e$ no longer increased the background leak $Na^+$ current, suggesting that activation of G protein by GTPγS suppressed the low-$[Ca^{2+}]_e$ activation of NALCN (Figure 8A). As a further test, we recorded the current with pipette solutions containing GDPβS, a nonhydrolyzable GDP analog that locks G-proteins in their inactive state. Upon break-in, an increase in holding current similar to that previously reported (Heuss et al., 1999) developed, even in the absence of $[Ca^{2+}]_e$ change. The current development was accompanied by an increase in input conductance, reflected by the current magnitudes from a ramp protocol, suggesting an activation of one or more channels (Figure 8B). Once this current reached plateau, reduction of $[Ca^{2+}]_e$ no longer activated additional current, suggesting that GDPβS and low-$[Ca^{2+}]_e$ acted on the same channel. In support of NALCN as the channel target, the GDPβS-activated current was absent in *nalcn*$^{-/-}$ neurons (Figures 8B and 8C), but could be restored by NALCN cDNA transfection (Figures 8D and 8E). Like the native current, the GDPβS-induced current was sensitive to $Gd^{3+}$ when restored with a wild-type NALCN (Figure 8D, left), but became resistant when restored with a $Gd^{3+}$-insensitive NALCN pore mutant (Figure 8D, right; EEKA motif in the pore instead of the wild-type EEKE [Lu et al., 2009]). Thus, the GDPβS-induced current is through the NALCN channel pore.

The involvement of G-proteins in $I_{NALCN}$'s $[Ca^{2+}]_e$ sensitivity suggests that the signal that activates NALCN upon a decrease in $[Ca^{2+}]_e$ is transmitted into cells through receptors coupled to the heterotrimeric G-proteins ($G_\alpha$ and $G_{\beta\gamma}$) or small G-proteins. In support of a role of the trimeric G-proteins, transfecting a constitutively active $G_{\alpha q}$ (Q209L) into wild-type neurons blocked $I_{LCA}$ (−13.8 ± 5.7 pA, n = 11; compared to −189.2 ± 38.8 pA, n = 17, from nontransfected control cells recorded in the same days) (Figures S5A and S5B).

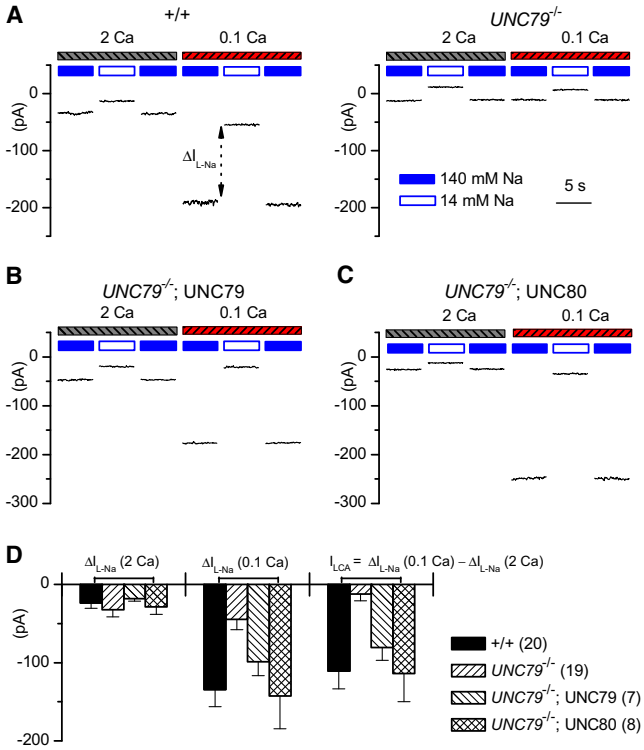


**Figure 6. The $Na^+$-Leak Current Is Insensitive to $[Ca^{2+}]_e$ in *unc79* Mutant Neurons, but the Sensitivity Can Be Rescued with UNC80**

(A–C) Representative $\Delta I_{L\text{-}Na}$ in wild-type (A, +/+), *unc79* knockout (A, *UNC79*$^{-/-}$), *unc79*$^{-/-}$ transfected with UNC79 cDNA (B), or *unc79*$^{-/-}$ transfected with UNC80 (C) neurons in baths containing 2 mM or 0.1 mM $Ca^{2+}$. (D) Summary of $\Delta I_{L\text{-}Na}$ recorded with 2 mM $[Ca^{2+}]_e$ (left group) and 0.1 mM $[Ca^{2+}]_e$ (middle group), and the difference between the two ($I_{LCA}$, right group). Neurons cultured from littermates under identical conditions were used for comparison between the wild-type and mutant. The number of cells for each condition is indicated in parentheses. Error bars represent mean and SEM.

### Coexpression of NALCN with UNC80 and a $Ca^{2+}$-Sensing G Protein-Coupled Receptor in HEK293T Cells Reconstitutes a $[Ca^{2+}]_e$-Sensitive NALCN Channel

Consistent with the possibility that CaSR, a $G_q$ G protein coupled receptor (GPCR) sensitive to $[Ca^{2+}]_e$ in the sub mM to mM range, or its homologs, might be the putative receptor sensing the $[Ca^{2+}]_e$ changes (Brown et al., 1995; Pi et al., 2005), $I_{LCA}$ could be inhibited by CaSR agonists spermidine and neomycin (Figure S5C; see also Formenti et al. [2001]).

Together, these data suggest that, in neurons, $I_{LCA}$ requires at least a channel-pore-forming protein, NALCN, an intracellular protein, UNC80, and a GPCR capable of sensing $[Ca^{2+}]_e$ changes. We next tested whether these three proteins together were able to reconstitute $I_{LCA}$ in HEK293T fibroblast cells, which do not have significant endogenous $I_{LCA}$ (Figures 9A and 9D). In HEK293T cells, transfection of NALCN alone generates $I_{NALCN}$ in cells with the highest level of expression (approximately the top 5%, as estimated by the intensity of green fluorescent protein encoded in the same vector [Lu et al., 2009]). Addition of UNC80 and a constitutively active Src kinase (Src529, bearing a Y529F mutation) increases the percentage of cells with detectable $I_{NALCN}$ to ~40% (Lu et al., 2009). $I_{NALCN}$ from these cells was insensitive to a reduction in $[Ca^{2+}]_e$ from 1.2 mM to 0.1 mM (Figures 9B and 9D). However, cotransfection with CaSR rendered the current sensitive to $[Ca^{2+}]_e$. The current was largely suppressed in the presence of 1.2 mM $[Ca^{2+}]_e$, but this suppression was released in response to a decrease in $[Ca^{2+}]_e$ to 0.1 mM (Figures 9C and 9D; Figure S6E). Similar to $I_{LCA}$ in neurons, the current reconstituted from CaSR, UNC80, and NALCN (Figure S6A), but not from the ones without CaSR (Figure S6B), was blocked by the CaSR agonist spermidine. Like in neurons, $I_{NALCN}$ reconstituted in the HEK293T cells with CaSR and UNC80 became insensitive to $[Ca^{2+}]_e$ when the C terminus of NALCN was deleted (Δ1638–1738) (Figures S6D and S6E).

## DISCUSSION

We have shown that $[Ca^{2+}]_e$ controls the size of NALCN channel currents in hippocampal neurons. This control appears to be a major mechanism by which a change in $[Ca^{2+}]_e$ around the physiological concentrations influences the resting excitability of the neurons. Thus, whereas extracellular $K^+$ may regulate neuronal excitability through many channels including the 15 two-pore domain $K^+$ leak channels (Goldstein et al., 2005), both $Na^+$ and $Ca^{2+}$ can exert their influence through the NALCN $Na^+$-leak channel, where $Ca^{2+}$ indirectly regulates the size of the NALCN current through a G protein-coupled receptor, which senses $[Ca^{2+}]_e$, and a G protein-dependent intracellular mechanism that couples the signal to the UNC79-UNC80-NALCN channel complex.

The ability of $Ca^{2+}$ to act as an intracellular messenger has been extensively studied at the molecular level, but the ion's potential role as an extracellular messenger is poorly understood. $[Ca^{2+}]_e$ has long been known to influence neuronal excitability (Frankenhaeuser and Hodgkin, 1957). Although $[Ca^{2+}]_e$ is considered relatively stable, it has been shown to fluctuate under conditions such as prolonged stimulation, or in microdomains, where extracellular space is limited, during physiological processes such as synaptic transmission and sleep, or pathophysiological conditions such as seizure and hypocalcemia. Artificially lowering $[Ca^{2+}]_e$ can induce seizure in intact animals and seizure-like activities in brain slices and single neurons (Feng and Durand, 2003; Kaczmarek and Adey, 1975). Neurons cultured from *nalcn*$^{-/-}$ and *unc79*$^{-/-}$ hippocampi are insensitive to the $[Ca^{2+}]_e$ drop from 1.2 mM to 0.5 or 0.1 mM, suggesting a major role of the NALCN complex in the low $[Ca^{2+}]_e$ –induced neuronal excitability. Other mechanisms, such as the charge screening effects and the TRPM7 channel (Hille, 2001; Wei et al., 2007), may play roles during more dramatic reduction of total extracellular divalent ions including $Mg^{2+}$. Future experiments, with a tissue-specific conditional knockout or a knockin to engineer animals with a $[Ca^{2+}]_e$-insensitive NALCN, will further define the in vivo roles of the regulation of NALCN by $[Ca^{2+}]_e$ in physiological functions, such as synaptic plasticity, and pathophysiological conditions such as seizure.

We have also uncovered several major components that appear to couple a drop in $[Ca^{2+}]_e$ to an opening of the channel: a $[Ca^{2+}]_e$-sensitive GPCR (CaSR), an UNC79-UNC80 complex, and the carboxy terminus of NALCN. These findings are

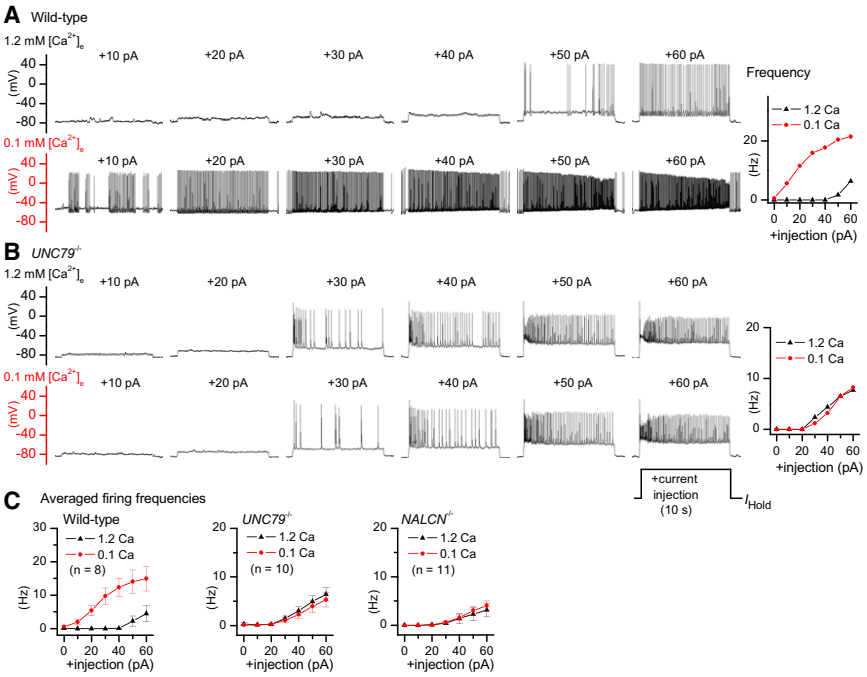


**Figure 7. Dependence of the Excitatory Action of Low $[Ca^{2+}]_e$ on UNC79**

Hyperpolarizing holding currents ($I_{Hold}$, −60 pA in the neuron in (A); −100 pA in (B); and −64.0 + 18.8 pA (wild-type), −83.7 + 19.2 pA (*unc79*$^{-/-}$) and −32.7 + 17.4 pA (*nalcn*$^{-/-}$) for (C) was injected to bring each neuron's steady membrane potential to −80 mV in 1.2 mM $Ca^{2+}$-containing bath. Pulses (10 s, as illustrated in lower right in (B)) of additional depolarizing currents with increasing amplitudes (+10 to +60 pA) were injected every 50 s. (A and B) Examples of current-clamp recordings from a wild-type (A) and an *unc79* mutant neuron (B) in baths containing 1.2 mM (upper traces) or 0.1 mM (lower traces) $Ca^{2+}$. Firing frequencies of the neurons during the 10 s depolarizing pulses are plotted in the right columns. Notice a large depolarization of holding membrane potential in the wild-type (A), but not in the mutant (B), when $[Ca^{2+}]_e$ was lowered to 0.1 mM. (C) Statistics of firing frequencies from wild-type (left), *unc79*$^{-/-}$ (middle), and *nacln*$^{-/-}$ (right) neurons. Some wild-type neurons became too depolarized in 0.1 mM $Ca^{2+}$-containing bath to have continuous firing, presumably because of inactivation of voltage-gated ion channels. These cells were not included in the analysis in (C). See also Figure S4. Error bars represent mean and SEM.

consistent with a model in which there is a tonic inhibition of NALCN current by a $[Ca^{2+}]_e$-sensing GPCR and where, in turn, lowering $[Ca^{2+}]_e$ releases the inhibition and thereby activates the channel (Figure S7). However, the precise mechanism by which a $[Ca^{2+}]_e$ signal is transmitted to the NALCN complex remains to be established. CaSR, other members in the Class C GPCR family such as GPRC6A (Pi et al., 2005), mGluR1 (Kubo et al., 1998), and $GABA_B$ (Wise et al., 1999), as well as the heterodimers among them (Gama et al., 2001) can all sense changes in both $[Ca^{2+}]_e$ and other stimuli such as amino acids (Hofer and Brown, 2003). The major known function of CaSR is to detect $[Ca^{2+}]_e$ in organs such as the parathyroid gland, which secretes parathyroid hormone to regulate systemic $Ca^{2+}$ levels (Hofer and Brown, 2003). Like NALCN, CaSR is also widely expressed in the brain, where it is found at particularly high levels in regions such as the hippocampus and cerebellum (Ruat et al., 1995). The neuronal function of CaSR is beginning to emerge: activated CaSR stimulates the dendritic growth of neurons (Vizard et al., 2008) and suppresses synaptic transmission (Phillips et al., 2008), although the mechanisms are largely unknown. Our findings suggest that CaSR or its homologs also play a role in the regulation of neuronal excitability. Many CaSR mutations are associated with epilepsy (Pidasheva et al., 2004). Future studies will examine whether CaSR may be involved in the interaction between UNC80 and the intracellular carboxy tail of NALCN, both of which are required for $I_{LCA}$.

We found that low $[Ca^{2+}]_e$ can act synergistically with the neuropeptide substance P to potentiate $I_{NALCN}$ in the hippocampal neurons (Figure 4). Similar synergism was also found between low $[Ca^{2+}]_e$ and the neuropeptide neurotensin in activating a cation current similar to $I_{NALCN}$ in midbrain dopaminergic neurons (Farkas et al., 1996). Although both the action of $[Ca^{2+}]_e$ and that of SP require UNC80, the signal transduction pathways underlying them are distinct. The $[Ca^{2+}]_e$ action through CaSR is dependent on G proteins and the last amino acids of the NALCN protein, whereas the effect of SP through TACR1 (the GPCR for SP) is independent of G proteins and the carboxy terminus of NALCN protein but requires the Src family of tyrosine-protein kinases (SFKs) (Lu et al., 2009). Single channel recording and protein trafficking studies of NALCN will be required to determine whether the two modes of action have distinct channel parameters, such as the number of channels (*N*) and the opening probability ($P_o$). $[Ca^{2+}]_e$ drop in brain regions occurs during seizure, where lowering $[Ca^{2+}]_e$ is enough to trigger seizure. Similarly, an increase of SP expression in the hippocampus has been observed in a model of status epilepticus, where it was proposed to be critical for the maintenance of the epilepticus state (Liu et al., 1999). A synergistic effect between $[Ca^{2+}]_e$ drop and Src kinases has also been observed in the "paradoxical" excitation of neurons and the increase of $[Ca^{2+}]_i$ by low $[Ca^{2+}]_e$ (Burgo et al., 2003). A simultaneous decrease in $[Ca^{2+}]_e$ and an activation of the kinases by neuropeptides and other stimuli would be expected to provide a powerful excitatory signal to the neurons through the synergistic activation of NALCN (Figure S7).

Our findings indicate that the NALCN complex contains at least three proteins: NALCN, UNC79, and UNC80, with a predicted total molecular weight of ~800 kDa (assuming a monomeric stoichiometry), a size larger than those of some of the $Na_V$s and $Ca_V$s (Arikkath and Campbell, 2003). Several lines of evidence support the possibility that UNC79 and UNC80 represent auxiliary subunits of the NALCN channel. First, the three proteins are physically associated. Second, UNC79 affects the UNC80 protein level (Figure 4). Third, UNC80 is required for

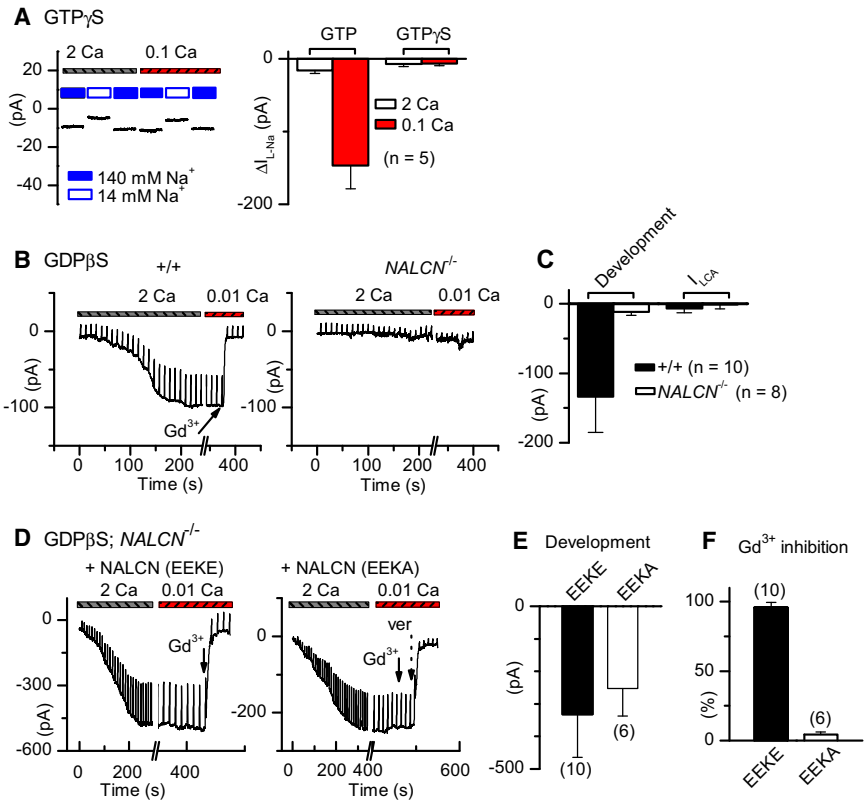


**Figure 8. $I_{LCA}$ Is G Protein-Dependent**

(A) Inclusion of GTPγS in the pipette solution blocked the low-$[Ca^{2+}]_e$ potentiation of the $Na^+$-leak current, as shown in a representative recording (left, >6 min after break-in), and summarized at right.

(B) In wild-type neurons (left), an inward current developed upon dialysis with pipette solution containing GDPβS ($V_h$ = −68 mV; gap-free recording with a ramp from −68 mV to −48 mV in 1.4 s, every 10.3 s). After the current reached a plateau (defined as current development), reduction of $[Ca^{2+}]_e$ no longer activated additional current. GDPβS did not activate current in a *nalcn*$^{-/-}$ neuron (right).

(C) Statistics of the GDPβS-activated current development, expressed as the size of the plateau current, and additional $I_{LCA}$ currents activated by lowering $[Ca^{2+}]_e$ to 0.01 mM in the presence of GDPβS, in the wild-type (+/+) and *nalcn*$^{-/-}$ mutant.

(D) Representative inward current development upon GDPβS dialysis in *nalcn*$^{-/-}$ neurons transfected with a wild-type NALCN ($Gd^{3+}$-sensitive; EEKE, left) or with a $Gd^{3+}$-resistant mutant (EEKA, right) NALCN. Note that lowering $[Ca^{2+}]_e$ did not activate further current in either cell. The EEKE- transfected neuron was blocked by 10 μM $Gd^{3+}$. The EEKA-transfected neuron was blocked by verapamil (ver, 1 mM, indicated by dashed arrow), but not by $Gd^{3+}$ (10 μM, indicated by solid arrow).

(E) Summary of the peak currents.

(F) Sensitivity to $Gd^{3+}$ (10 μM) blockade. See also Figure S5. Error bars represent mean and SEM.

the control of the NALCN channel by GPCRs (Figure 6 and Lu et al. [2009]). Fourth, mutations in *unc79*, *unc80*, and *nalcn* have similar phenotypes, which are in turn similar to the double mutant phenotype (Humphrey et al., 2007; Jospin et al., 2007; Nakayama et al., 2006; Yeh et al., 2008), suggesting that the major roles of UNC79/UNC80 are NALCN-related.

The sizes of the basal leak currents ($I_{L\text{-}Na}$) in WT and *unc79* KO neurons were comparable (Figure 6D). Overexpression of NALCN in the *unc79* mutant background actually generated a leak current larger than that in the wild-type (not shown). Although, because the antibodies we developed do not optimally recognize native proteins in immunocytochemical preparations, we cannot exclude the possibility that NALCN has a different localization in the *unc79* mutant, these data are consistent with our previous findings that NALCN can form an ion channel without an apparent requirement for UNC79 (Lu et al., 2007; Lu et al., 2009). Our preliminary studies did not observe an obvious influence of UNC79 on properties of NALCN expressed in HEK293T cells. Further studies may need to examine if UNC79 influences the more subtle characteristics of the channel. Both *unc79* and *nalcn* knockout mice have disrupted breathing rhythms, fail to nurse, and die as neonates ((Lu et al., 2007; Nakayama et al., 2006), and unpublished observations). Some *unc79* KO mice survive beyond the first day, whereas *nalcn* KO mice die within 24 hr of birth. The slightly weaker phenotype of *unc79* KOs apparently reflects the function of the basal leak current through NALCN without UNC79/UNC80. However, it is clear that this current is not sufficient to support the animal's viability. One possible reason for the residual current's inability to support life is that its localization may be defective in the *unc79* mutant. Another possibility is that the ability of NALCN to be activated or suppressed by GPCRs, which is dependent on the presence of UNC80 missing in the *unc79* mutant, is critical to survival. It has been proposed that activation of background currents similar to $I_{NALCN}$ by neurotransmitters may be critical to the generation of respiratory rhythms in the brainstem, such that modulation of the $Na^+$-leak may play a fundamental role (Ptak et al., 2009).

In summary, we have uncovered a novel molecular mechanism by which extracellular $Ca^{2+}$ ion influences the resting excitability of neurons. The signaling cascade includes a GPCR that senses $[Ca^{2+}]_e$ change and transmits the signal into the cell, as well as an UNC79/UNC80 complex that may couple the signal to the NALCN carboxy terminus. This regulatory pathway also interacts with a G protein-independent mode of control by neuropeptides. NALCN does not inactivate and is $Na^+$-permeable. Control of the UNC79-UNC80-NALCN channel complex represents a powerful mechanism to influence neuronal excitability.

## EXPERIMENTAL PROCEDURES

### Animals

Animal use was in accordance with protocols approved by the University of Pennsylvania IACUC. The generation of *nalcn* (Lu et al., 2007) and *unc79*

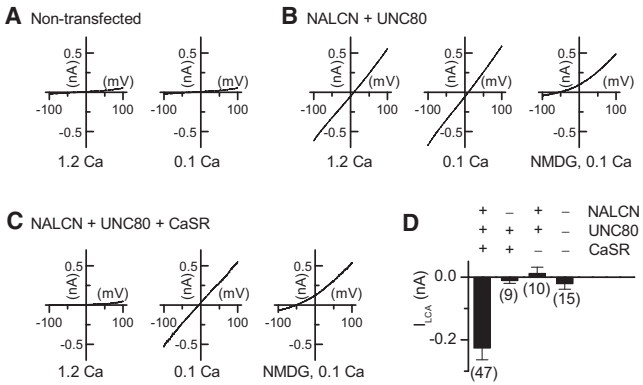


**Figure 9. Reconstitution of a $[Ca^{2+}]_e$-Sensitive NALCN Current in HEK293T Fibroblasts with CaSR, NALCN, and UNC80**

(A–C) Representative currents obtained with a voltage- ramp protocol (−100 mV to +100 mV in 1 s, Vh = −20 mV) from nontransfected cells (A) or cells transfected with various combination of NALCN, UNC80, and CaSR, as indicated (B and C) in baths containing 1.2 mM $Ca^{2+}$ (1.2 Ca) or 0.1 mM $Ca^{2+}$ (0.1 Ca). All baths contained 155 mM $Na^+$ except that $NMDG^+$ was used to replace $Na^+$ and $K^+$ in the (NMDG, 0.1 Ca) baths. All transfections also included a constitutively active Src (Src529) to increase the percentage of cells expressing detectable current (see Experimental Procedures and Lu et al. [2009]).

(D) Averaged size of the increase of inward current ($I_{LCA}$, at −100 mV) upon lowering $[Ca^{2+}]_e$ from 1.2 mM to 0.1 mM ($I_{LCA}$). Cell number for each experiment is shown in parentheses. See also Figure S6. Error bars represent mean and SEM.

(other name KIAA1409) (Nakayama et al., 2006) knockout mice has been previously described. Mice were derived from heterozygous matings in lines that had been backcrossed to C57BL/6 for more than 10 generations.

### Cloning of Full-Length UNC79

The full-length mouse cDNA clone used in this study was assembled in a pcDNA3.1-based vector from three fragments, each of which had been PCR-amplified from mouse brain cDNA with primers designed from partial sequences predicted based on *Drosophila* UNC79 sequences. All fragments used to assemble the full-length clones were sequenced to ensure that no sequence errors had been introduced during amplification. The human UNC79 full-length clone was assembled from an EST clone containing part of the ORF (GenBank accession number AB037830, a gift from Kazusa DNA Research Institute) and a fragment obtained using 5′RACE from a human brain cDNA library. Sequences of the mouse UNC79 clone have been deposited in GenBank (GQ334471). The mouse clone was used for the patch clamp experiments. In some protein chemistry experiments (Figure 5), the human UNC79 (94% identical with the mouse one) was used, and the interaction was also confirmed with the mouse clone.

### Cell Culture and DNA Transfection

Hippocampal neurons, dissociated from (postnatal day) P0 mouse brains, were digested with papain and plated on poly-L-lysine-coated glass coverslips (12- or 5-mm diameter) in 35-mm dishes at ~3–4 × $10^5$ cells/dish. The starting medium consisted of 80% DMEM (Lonza), 10% Ham's F-12 (Lonza), 10% bovine calf serum (iron supplemented, Hyclone) and 0.5 × penicillin-streptomycin (Invitrogen). Cells were changed the next day (DIV 1) to Neurobasal A medium (GIBCO) supplemented with 2% B-27, 0.5 × penicillin/streptomycin, and 1 × Glutamax. Cultures were maintained in a 37°C humidified incubator at 5% $CO_2$. For some experiments (Figures 2, 4, and 8), the neurons (1.5–2 × $10^5$ cells/dish) were plated onto glia-preplated coverslips or dishes, and maintained in the starting medium. Neurons cultured under this condition are known to have a more robust SP-activated current (Lu et al., 2009). When necessary, cytosine-arabinofuranoside (Sigma) was added at 6 μM to suppress glial growth. Neurons were recorded between DIV 7 and 18. At least 1 day before the experiment, two-thirds of the medium was replaced with fresh medium without glial inhibitor and antibiotics.

The SH-SY5Y human neuroblastoma cell line was cultured in 1:1 DMEM /F-12 (GIBCO) supplemented with 10% FBS and 1 × penicillin-streptomycin. HEK293T fibroblasts were cultured in DMEM (GIBCO) supplemented with 10% FBS, 1 × Glutamax and 1 × Penn/Strep. The cultures were kept in 37°C in a humidified 5% $CO_2$ atmosphere.

For transfection experiments, Lipofectamine 2000 was used as the transfection reagent. Neurons between DIV 5 and 7 were used for transfection. The transfected SH-SY5Y and HEK293T cells were replated the day before (for SH-SY5Y) or on the day of (for HEK293T cells) recording. Recordings were done 48-72 hr (for HEK293T cells) or 48–60 hr (for the other) after transfection. Transfected cells were identified using the GFP and/or RFP marker.

### Immunoprecipitation and Western Blotting

The anti-NALCN and anti-UNC80 antibodies used in this study have been previously described (Lu et al., 2009). The polyclonal anti-UNC79 antibody was generated in rabbit with a KLH-conjugated peptide (sequence, CQVEIQSSEAASQFYPL) derived from the carboxy-terminus, and was affinity-purified with the peptide.

For HEK293T cells, cells were lysed by incubation at 4°C for 1 hr in RIPA buffer (50 mM Tris-HCl, 150 mM NaCl, 1% NP-40, 0.5% (w/v) deoxycholate, 0.1% (w/v) SDS, pH 7.4) supplemented with a protease inhibitor cocktail (PIC). After centrifuging for 30 min at 20,000 × g, the supernatants were mixed with immunoprecipitating antibodies and incubated at 4°C for 2 hr. Samples were then mixed with buffer-equilibrated protein A-agarose at 4°C for 2–14 hr. After three 10 min washes with RIPA buffer, bound proteins were eluted with a lithium dodecyl sulfate (LDS) sample buffer.

For brain proteins, frozen adult (Figure 5A) or newborn (Figures 5C–5E) brains were powdered in dry ice and homogenized in RIPA buffer with PIC. The homogenates were then solubilized at 4°C for 30 min. After centrifuging at 20,000 × g for 30 min, the supernatants were either used immediately for immunoprecipitation or stored at −80°C for later use. One mg of total protein was precipitated with 1 μg of antibody.

Protein electrophoresis was performed with 4%–12% Bis-Tris gradient gels in MOPS-SDS running buffer (Invitrogen). Proteins were transferred onto polyvinylidene diflouride (PVDF) membranes. After being blocked with 5% nonfat dry milk in PBS with 0.1% Tween-20 (PBST), membranes were incubated with primary antibodies at 4°C overnight or, for anti-Flag, at room temperature for 2 hr. After incubation with horseradish-peroxidase-labeled secondary antibodies for 1 hr at room temperature, membranes were developed with SuperSignal West Pico ECL or SuperSignal West Dura ECL.

### Patch Clamp Analysis Using Hippocampal Neurons and SH-SY5Y Cells

All recordings were carried out at room temperature (20–25°C). Pyramidal neurons morphologically identified were used for neuronal recordings. For voltage-clamp experiments, the standard pipette solution contained 120 mM CsCl, 4 mM EGTA, 2 mM $CaCl_2$, 2 mM $MgCl_2$, 10 mM HEPES, 4 mM Mg-ATP, 0.3 mM Tris-GTP, and 14 mM phosphocreatine (di-tris salt) (pH adjusted to 7.4 with CsOH; ~300 mOsm/L; intracellular free $[Ca^{2+}]$ of ~60 nM and $[Mg^{2+}]$ of ~2 mM, estimated with WEBMAXC). GTP was omitted in pipette solution containing GTPγS (1.5 mM) or GDPβS (1 mM). The bath solution contained 140 mM NaCl, 5 mM KCl, 1 mM $MgCl_2$, 10 mM HEPES, 2 mM CsCl, 6 mM glucose, and $CaCl_2$ (2 mM unless otherwise indicated) (pH 7.4 with Tris-OH, ~315 mOsm/L). Tris-Cl was used to replace 126 mM NaCl in the baths containing 14 mM $Na^+$ bath. Similar results were obtained when NMDG was used to replace $Na^+$. TTX (1 μM) and ABC mix (10 μM APV, 20 μM bicuculline, 20 μM CNQX) were applied in the bath to block $Na_v$ and synaptic currents. The $I_{L\text{-}Na}$ leak current was measured by subtracting the currents recorded in low (14 mM) $[Na^+]_e$ from those in high (140 mM) $[Na^+]_e$ at holding potentials ($\Delta I_{L\text{-}Na}$) (Lu et al., 2007). For $\Delta I_{L\text{-}Na}$ measurement, special precaution was taken to ensure that the current was not a result of recording instability. After recording in a bath containing different $[Na^+]_e$, the bath was perfused back to the original $[Na^+]_e$. Only those with a fluctuation of the holding current change below 5 pA or 20% of $\Delta I_{L\text{-}Na}$ between the first and the last baths, with the same $[Na^+]_e$,

were used for further analysis. In some initial experiments used in Figure 2, $\Delta I_{L\text{-}Na}$ was measured with a $K^+$-containing pipette solution as described before (Lu et al., 2007). The low $[Ca^{2+}]_e$-activated current, $I_{LCA}$, was measured as the change in the size of $\Delta I_{L\text{-}Na}$ or the change of the holding current (in bath containing 140 mM $Na^+$) when $[Ca^{2+}]_e$ was lowered as indicated. When $I_{LCA}$ was measured as the holding current change (in Figures 4, 8, and 9), either blockers or $[Na^+]_e$ reduction was applied to ensure that the current used for analysis was not due to nonspecific leak.

For current-clamp recordings, the pipette solution contained 135 mM K-Asp, 5 mM NaCl, 5 mM KCl, 2 mM $MgCl_2$, 1 mM EGTA, 10 mM HEPES, 4 mM Mg-ATP, 0.3 mM Tris-GTP, 14 mM phosphocreatine (di-tris) (pH 7.4 with KOH). The bath solution contained 150 mM NaCl, 3.5 mM KCl, 1 mM $MgCl_2$, 10 mM HEPES, 20 mM glucose, and $CaCl_2$ at the indicated concentration (pH 7.4 with 5 NaOH, ~320 mOsm/L). Neurons were isolated with APV (10 μM), bicuculline (20 μM) and CNQX (20 μM).

### Patch Clamp Analyses Using HEK293T Cells

The pipette solution contained 150 mM Cs, 120 mM Mes, 10 mM NaCl, 10 mM EGTA, 4 mM $CaCl_2$, 0.3 mM $Na_2GTP$, 2 mM Mg-ATP, 10 mM HEPES (pH 7.4, ~300 mOsm/L). Bath solutions contained 150 mM NaCl, 3.5 mM KCl, 1 mM $MgCl_2$, 10 mM HEPES, 20 mM glucose, and $CaCl_2$ at the indicated concentrations (pH 7.4 with 5 mM NaOH, ~320 mOsm/L). In the NMDG bath, $Na^+$ and $K^+$ were replaced by $NMDG^+$. In the $I_{LCA}$ reconstitution experiments, 0.5 μg NALCN, 0.5 μg UNC80, 0.5 μg Src529, and 2 μg CaSR cDNA were cotransfected. The NALCN and CaSR constructs were made in vectors based on pTracer-CMV2 (Invitrogen) modified to also express eGFP (for NALCN) or mCherry RFP (for CaSR) under a separate promoter. The human CaSR insert was from an IMAGE EST clone (ID #8327704). Only cells with moderate level of both GFP and RFP fluorescence signals were selected for recordings. In control experiments where one or more constructs were not included, an equal amount of empty vector DNA was used to ensure that all the transfections contained the same amount of DNA.

Liquid junction potentials (estimated using Clampex software) were corrected offline. Patch clamp recordings were performed using an Axopatch-200A amplifier controlled with Clampex 9.2 or Clampex 10 software (Axon). Signals were digitized at 2–10 kHz with a Digidata 1322A or 1440 digitizer.

## ACCESSION NUMBERS

Sequences of the mouse UNC79 clone have been deposited in GenBank under accession number GQ334471.

## SUPPLEMENTAL INFORMATION

Supplemental Information includes seven figures and can be found with this article online at doi:10.1016/j.neuron.2010.09.014.

## ACKNOWLEDGMENTS

We thank Drs. Bruce Bean, Kevin Foskett, Igor Medina, Betsy Navarro, and Haoxing Xu for critically reading earlier versions of the manuscript and suggestions, Lixia Yue for cDNA clones, and members of the Ren lab for help in experiments and discussion. This work was supported by grants from the American Heart Association and the National Institutes of Health.

Accepted: August 27, 2010
Published: November 3, 2010

## REFERENCES

Almers, W., and McCleskey, E.W. (1984). Non-selective conductance in calcium channels of frog muscle: Calcium selectivity in a single-file pore. J. Physiol. *353*, 585–608.

Amzica, F., Massimini, M., and Manfridi, A. (2002). Spatial buffering during slow and paroxysmal sleep oscillations in cortical networks of glial cells in vivo. J. Neurosci. *22*, 1042–1053.

Arikkath, J., and Campbell, K.P. (2003). Auxiliary subunits: Essential components of the voltage-gated calcium channel complex. Curr. Opin. Neurobiol. *13*, 298–307.

Armstrong, C.M., and Cota, G. (1991). Calcium ion as a cofactor in Na channel gating. Proc. Natl. Acad. Sci. USA *88*, 6528–6531.

Benninger, C., Kadis, J., and Prince, D.A. (1980). Extracellular calcium and potassium changes in hippocampal slices. Brain Res. *187*, 165–182.

Borst, J.G., and Sakmann, B. (1999). Depletion of calcium in the synaptic cleft of a calyx-type synapse in the rat brainstem. J. Physiol. *521*, 123–133.

Brown, E.M., Pollak, M., Seidman, C.E., Seidman, J.G., Chou, Y.H., Riccardi, D., and Hebert, S.C. (1995). Calcium-ion-sensing cell-surface receptors. N. Engl. J. Med. *333*, 234–240.

Burgo, A., Carmignoto, G., Pizzo, P., Pozzan, T., and Fasolato, C. (2003). Paradoxical $Ca^{2+}$ rises induced by low external $Ca^{2+}$ in rat hippocampal neurones. J. Physiol. *549*, 537–552.

Chinopoulos, C., Connor, J.A., and Shuttleworth, C.W. (2007). Emergence of a spermine-sensitive, non-inactivating conductance in mature hippocampal CA1 pyramidal neurons upon reduction of extracellular $Ca^{2+}$: Dependence on intracellular $Mg^{2+}$ and ATP. Neurochem. Int. *50*, 148–158.

Clapham, D.E. (2007). Calcium signaling. Cell *131*, 1047–1058.

Farkas, R.H., Chien, P.Y., Nakajima, S., and Nakajima, Y. (1996). Properties of a slow nonselective cation conductance modulated by neurotensin and other neurotransmitters in midbrain dopaminergic neurons. J. Neurophysiol. *76*, 1968–1981.

Feng, Z., and Durand, D.M. (2003). Low-calcium epileptiform activity in the hippocampus in vivo. J. Neurophysiol. *90*, 2253–2260.

Formenti, A., De Simoni, A., Arrigoni, E., and Martina, M. (2001). Changes in extracellular $Ca^{2+}$ can affect the pattern of discharge in rat thalamic neurons. J. Physiol. *535*, 33–45.

Frankenhaeuser, B., and Hodgkin, A.L. (1957). The action of calcium on the electrical properties of squid axons. J. Physiol. *137*, 218–244.

Gama, L., Wilt, S.G., and Breitwieser, G.E. (2001). Heterodimerization of calcium sensing receptors with metabotropic glutamate receptors in neurons. J. Biol. Chem. *276*, 39053–39059.

Goldstein, S.A., Bayliss, D.A., Kim, D., Lesage, F., Plant, L.D., and Rajan, S. (2005). International Union of Pharmacology. LV. Nomenclature and molecular relationships of two-P potassium channels. Pharmacol. Rev. *57*, 527–540.

Hablitz, J.J., Heinemann, U., and Lux, H.D. (1986). Step reductions in extracellular $Ca^{2+}$ activate a transient inward current in chick dorsal root ganglion cells. Biophys. J. *50*, 753–757.

Heinemann, U., Konnerth, A., Pumain, R., and Wadman, W.J. (1986). Extracellular calcium and potassium concentration changes in chronic epileptic brain tissue. Adv. Neurol. *44*, 641–661.

Heinemann, U., and Pumain, R. (1980). Extracellular calcium activity changes in cat sensorimotor cortex induced by iontophoretic application of amino acids. Exp. Brain Res. *40*, 247–250.

Hess, P., Lansman, J.B., and Tsien, R.W. (1986). Calcium channel selectivity for divalent and monovalent cations. Voltage and concentration dependence of single channel current in ventricular heart cells. J. Gen. Physiol. *88*, 293–319.

Heuss, C., Scanziani, M., Gahwiler, B.H., and Gerber, U. (1999). G-protein-independent signaling mediated by metabotropic glutamate receptors. Nat. Neurosci. *2*, 1070–1077.

Hille, B. (2001). Ion Channels of Excitable Membranes, Third Edition (Sunderland, MA: Sinauer Associates, Inc.).

Hodgkin, A.L., and Katz, B. (1949). The effect of sodium ions on the electrical activity of the giant axon of the squid. J. Physiol. *108*, 37–77.

Hofer, A.M., and Brown, E.M. (2003). Extracellular calcium sensing and signalling. Nat. Rev. Mol. Cell Biol. *4*, 530–538.

Humphrey, J.A., Hamming, K.S., Thacker, C.M., Scott, R.L., Sedensky, M.M., Snutch, T.P., Morgan, P.G., and Nash, H.A. (2007). A putative cation channel and its novel regulator: Cross-species conservation of effects on general anesthesia. Curr. Biol. *17*, 624–629.

Jospin, M., Watanabe, S., Joshi, D., Young, S., Hamming, K., Thacker, C., Snutch, T., Jorgensen, E., and Schuske, K. (2007). UNC-80 and the NCA ion channels contribute to endocytosis defects in synaptojanin mutants. Curr. Biol. *17*, 1595–1600.

Kaczmarek, L.K., and Adey, W.R. (1975). Extracellular release of cerebral macromolecules during potassium- and low-calcium-induced seizures. Epilepsia *16*, 91–97.

Kozak, J.A., and Cahalan, M.D. (2003). MIC channels are inhibited by internal divalent cations but not ATP. Biophys. J. *84*, 922–927.

Krnjevic, K., Morris, M.E., Reiffenstein, R.J., and Ropert, N. (1982). Depth distribution and mechanism of changes in extracellular $K^+$ and $Ca^{2+}$ concentrations in the hippocampus. Can. J. Physiol. Pharmacol. *60*, 1658–1671.

Kubo, Y., Miyashita, T., and Murata, Y. (1998). Structural basis for a $Ca^{2+}$-sensing function of the metabotropic glutamate receptors. Science *279*, 1722–1725.

Lee, J.H., Cribbs, L.L., and Perez-Reyes, E. (1999). Cloning of a novel four repeat protein related to voltage-gated sodium and calcium channels. FEBS Lett. *445*, 231–236.

Liu, H., Mazarati, A.M., Katsumori, H., Sankar, R., and Wasterlain, C.G. (1999). Substance P is expressed in hippocampal principal neurons during status epilepticus and plays a critical role in the maintenance of status epilepticus. Proc. Natl. Acad. Sci. USA *96*, 5286–5291.

Liu, J., Xia, J., Cho, K.H., Clapham, D.E., and Ren, D. (2007). CatSperbeta, a novel transmembrane protein in the CatSper channel complex. J. Biol. Chem. *282*, 18945–18952.

Lu, B., Su, Y., Das, S., Liu, J., Xia, J., and Ren, D. (2007). The neuronal NALCN channel contributes resting sodium permeability and is required for normal respiratory rhythm. Cell *129*, 371–383.

Lu, B., Su, Y., Das, S., Wang, H., Wang, Y., Liu, J., and Ren, D. (2009). Peptide neurotransmitters activate a cation channel complex of NALCN and UNC-80. Nature *457*, 741–744.

MacDonald, J.F., Xiong, Z.G., and Jackson, M.F. (2006). Paradox of $Ca^{2+}$ signaling, cell death and stroke. Trends Neurosci. *29*, 75–81.

Monteilh-Zoller, M.K., Hermosura, M.C., Nadler, M.J., Scharenberg, A.M., Penner, R., and Fleig, A. (2003). TRPM7 provides an ion channel mechanism for cellular entry of trace metal ions. J. Gen. Physiol. *121*, 49–60.

Morris, M.E., and Trippenbach, T. (1993). Changes in extracellular $[K^+]$ and $[Ca^{2+}]$ induced by anoxia in neonatal rabbit medulla. Am. J. Physiol. *264*, R761–R769.

Nadler, M.J., Hermosura, M.C., Inabe, K., Perraud, A.L., Zhu, Q., Stokes, A.J., Kurosaki, T., Kinet, J.P., Penner, R., Scharenberg, A.M., and Fleig, A. (2001). LTRPC7 is a Mg.ATP-regulated divalent cation channel required for cell viability. Nature *411*, 590–595.

Nakayama, M., Iida, M., Koseki, H., and Ohara, O. (2006). A gene-targeting approach for functional characterization of KIAA genes encoding extremely large proteins. FASEB J. *20*, 1718–1720.

Nicholls, J.G., Martin, A.R., Wallace, B.G., and Fuchs, P.A. (2001). From Neuron to Brain, Fourth Edition (Sunderland, MA: Sinauer Associates, Inc.).

Nicholson, C., Bruggencate, G.T., Steinberg, R., and Stockle, H. (1977). Calcium modulation in brain extracellular microenvironment demonstrated with ion-selective micropipette. Proc. Natl. Acad. Sci. USA *74*, 1287–1290.

Nilsson, P., Hillered, L., Olsson, Y., Sheardown, M.J., and Hansen, A.J. (1993). Regional changes in interstitial $K^+$ and $Ca^{2+}$ levels following cortical compression contusion trauma in rats. J. Cereb. Blood Flow Metab. *13*, 183–192.

Owsianik, G., Talavera, K., Voets, T., and Nilius, B. (2006). Permeation and selectivity of TRP channels. Annu. Rev. Physiol. *68*, 685–717.

Phillips, C.G., Harnett, M.T., Chen, W., and Smith, S.M. (2008). Calcium-sensing receptor activation depresses synaptic transmission. J. Neurosci. *28*, 12062–12070.

Pi, M., Faber, P., Ekema, G., Jackson, P.D., Ting, A., Wang, N., Fontilla-Poole, M., Mays, R.W., Brunden, K.R., Harrington, J.J., and Quarles, L.D. (2005). Identification of a novel extracellular cation-sensing G-protein-coupled receptor. J. Biol. Chem. *280*, 40201–40209.

Pidasheva, S., D'Souza-Li, L., Canaff, L., Cole, D.E., and Hendy, G.N. (2004). CASRdb: Calcium-sensing receptor locus-specific database for mutations causing familial (benign) hypocalciuric hypercalcemia, neonatal severe hyperparathyroidism, and autosomal dominant hypocalcemia. Hum. Mutat. *24*, 107–111.

Pierce-Shimomura, J.T., Chen, B.L., Mun, J.J., Ho, R., Sarkis, R., and McIntyre, S.L. (2008). Genetic analysis of crawling and swimming locomotory pattern in C. elegans. Proc. Natl. Acad. Sci. USA *105*, 20982–20987.

Ptak, K., Yamanishi, T., Aungst, J., Milescu, L.S., Zhang, R., Richerson, G.B., and Smith, J.C. (2009). Raphé neurons stimulate respiratory circuit activity by multiple mechanisms via endogenously released serotonin and substance P. J. Neurosci. *29*, 3720–3737.

Pumain, R., Menini, C., Heinemann, U., Louvel, J., and Silva-Barrat, C. (1985). Chemical synaptic transmission is not necessary for epileptic seizures to persist in the baboon Papio papio. Exp. Neurol. *89*, 250–258.

Ruat, M., Molliver, M.E., Snowman, A.M., and Snyder, S.H. (1995). Calcium sensing receptor: Molecular cloning in rat and localization to nerve terminals. Proc. Natl. Acad. Sci. USA *92*, 3161–3165.

Runnels, L.W., Yue, L., and Clapham, D.E. (2001). TRP-PLIK, a bifunctional protein with kinase and ion channel activities. Science *291*, 1043–1047.

Rusakov, D.A., and Fine, A. (2003). Extracellular $Ca^{2+}$ depletion contributes to fast activity-dependent modulation of synaptic transmission in the brain. Neuron *37*, 287–297.

Silver, I.A., and Erecinska, M. (1990). Intracellular and extracellular changes of $[Ca^{2+}]$ in hypoxia and ischemia in rat brain in vivo. J. Gen. Physiol. *95*, 837–866.

Smith, S.M., Bergsman, J.B., Harata, N.C., Scheller, R.H., and Tsien, R.W. (2004). Recordings from single neocortical nerve terminals reveal a nonselective cation channel activated by decreases in extracellular calcium. Neuron *41*, 243–256.

Snutch, T.P., and Monteil, A. (2007). The sodium "leak" has finally been plugged. Neuron *54*, 505–507.

Stanley, E.F. (2000). Presynaptic calcium channels and the depletion of synaptic cleft calcium ions. J. Neurophysiol. *83*, 477–482.

Vizard, T.N., O'Keeffe, G.W., Gutierrez, H., Kos, C.H., Riccardi, D., and Davies, A.M. (2008). Regulation of axonal and dendritic growth by the extracellular calcium-sensing receptor. Nat. Neurosci. *11*, 285–291.

Wang, H., Liu, J., Cho, K.H., and Ren, D. (2009). A novel, single transmembrane protein CATSPERG is associated with mouse CATSPER1 channel protein. Biol. Reprod. *81*, 539–544.

Wei, W.L., Sun, H.S., Olah, M.E., Sun, X., Czerwinska, E., Czerwinski, W., Mori, Y., Orser, B.A., Xiong, Z.G., Jackson, M.F., et al. (2007). TRPM7 channels in hippocampal neurons detect levels of extracellular divalent cations. Proc. Natl. Acad. Sci. USA *104*, 16323–16328.

Wise, A., Green, A., Main, M.J., Wilson, R., Fraser, N., and Marshall, F.H. (1999). Calcium sensing properties of the GABA(B) receptor. Neuropharmacology *38*, 1647–1656.

Xiong, Z., Lu, W., and MacDonald, J.F. (1997). Extracellular calcium sensed by a novel cation channel in hippocampal neurons. Proc. Natl. Acad. Sci. USA *94*, 7012–7017.

Yang, J., Ellinor, P.T., Sather, W.A., Zhang, J.F., and Tsien, R.W. (1993). Molecular determinants of $Ca^{2+}$ selectivity and ion permeation in L-type $Ca^{2+}$ channels. Nature *366*, 158–161.

Yeh, E., Ng, S., Zhang, M., Bouhours, M., Wang, Y., Wang, M., Hung, W., Aoyagi, K., Melnik-Martinez, K., Li, M., et al. (2008). A putative cation channel, NCA-1, and a novel protein, UNC-80, transmit neuronal activity in C. elegans. PLoS Biol. *6*, e55.

Yu, F.H., Yarov-Yarovoy, V., Gutman, G.A., and Catterall, W.A. (2005). Overview of molecular relationships in the voltage-gated ion channel superfamily. Pharmacol. Rev. *57*, 387–395.